Journal of Materials Chemistry A

PAPER

View Article Online
View Journal | View Issue



Cite this: J. Mater. Chem. A, 2014, 2, 10639

# How to repel hot water from a superhydrophobic surface?†

Zhe-Jun Yu,[a] Jieyi Yang,‡[b] Fang Wan,[a] Quan Ge,[a] Long-Lai Yang,[a] Zun-Liang Ding,[a] De-Quan Yang,*[a] Edward Sacher[c] and Tayirjan T. Isimjan[d]

Superhydrophobic surfaces, with water contact angles greater than 150° and slide angles less than 10°, have attracted a great deal of attention due to their self-cleaning ability and excellent water-repellency. It is commonly accepted that a superhydrophobic surface loses its superhydrophobicity in contact with water hotter than 50 °C. Such a phenomenon was recently demonstrated by Liu *et al.* [*J. Mater. Chem.*, 2009, **19**, 5602], using both natural lotus leaf and artificial leaf-like surfaces. However, our work has shown that superhydrophobic surfaces maintained their superhydrophobicity, even in water at 80 °C, provided that the leaf temperature is greater than that of the water droplet. In this paper, we report on the wettability of water droplets on superhydrophobic thin films, as a function of both their temperatures. The results have shown that both the water contact and slide angles on the surfaces will remain unchanged when the temperature of the water droplet is greater than that of the surface. The water contact angle, or the slide angle, will decrease or increase, however, with droplet temperatures increasingly greater than that of the surfaces. We propose that, in such cases, the loss of superhydrophobicity of the surfaces is caused by evaporation of the hot water molecules and their condensation on the cooler surface.

Received 20th February 2014
Accepted 30th April 2014

DOI: 10.1039/c4ta00882k

www.rsc.org/MaterialsA

## Introduction

Superhydrophobic surfaces, including thin films, coatings and surface modifications, have attracted a great deal of attention in academia and industry.[1] Their preparation, characterization and applications have been extensively reviewed.[2–4] However, most of these studies used water and substrates at room temperature to evaluate wettability. Typically, a superhydrophobic surface implies a surface of water contact angles greater than 150° and slide angles less than 10°. The wettability of a solid surface is controlled by both its chemical composition and its surface roughness.

Several reports exist on the water repelling properties of superhydrophobic surfaces to water at temperatures greater than 50°. Xia *et al.*[5] reported the fabrication of multi-responsive surfaces, which can change their wettabilities between superhydrophobic and superhydrophilic in response to temperature, pH, and glucose. These surfaces, even when heated to 55 °C, possessed high water-contact angles to cold water. He *et al.*[6] studied the superhydrophobicity of surfaces around the dew-point, using a superhydrophobic surface of poly(dimethylsiloxane) (PDMS) post-arrays, prepared using a porous silicon template. They found that the contact angle of water with all the surfaces decreases, when the surface temperature, within 20 °C, decreases to approach the dew-point. The water contact angles of these surfaces are still greater than 150° when the area fractions of the solid surface in contact with the liquid are ≤0.068.

Liu *et al.*[7] recently reported the wettability of several superhydrophobic surfaces, including lotus leaves, Teflon, silica–fluoropolymer composites and sol–gel processes, on silicon wafers at room temperature, using water at 50–80 °C. They demonstrated that water contact angles decreased markedly in hot water. This led to their conclusion that, while the wettability

[a]Materials Research Lab., Wuxi Shunye Technology Co., Ltd., 29# Lianze Road, Shanshui Cheng Tech. Park, Suite 15, Binhu District, Wuxi, Jiangsu, 214125, China. E-mail: dequan.yang@gmail.com; Tel: +86-510-6668-5886

[b]Department of Biochemistry, Rosalind and Morris Goodman Cancer Research Centre, McGill University, 1160 Pine Ave. West, Montreal, Quebec, H3A 1A3, Canada

[c]Laboratory for the Analysis of the Surfaces of Materials, Department of Engineering Physics, École Polytechnique de Montreal, Case Postale 6079, succursale Centre-Ville, Montreal, Québec H3C 3A7, Canada

[d]Division of Physical Sciences and Engineering, Solar and Photvoltaics Engineering Center, King Abdullah University of Science and Technology (KAUST), Thuwal 23955-6900, Saudi Arabia

† Electronic supplementary information (ESI) available: Fig. S1 and S2 are, respectively, the water contact angle measurement setup and a description of the method. Fig. S3 contains photographs of poinsettia leaf parts used for the WCA measurements. Fig. S4 contains SEM photomicrographs of the poinsettia surface: bare, and contacted with water at 30° and 80 °C. Fig. S5 shows XPS survey spectra of the superhydrophobic surfaces. Fig. S6 shows the high resolution C1s XPS spectra of the samples. There is also a video showing fog formation on the superhydrophobic surface (the transparent superhydrophobic coating on a truck mirror) on the water droplet leaving at water temperature higher (16 °C) than the surface temperature (12 °C). See DOI: 10.1039/c4ta00882k

‡ Summer student.

of a solid surface is governed by both surface roughness and surface free energy, the surface energy is more significant than its roughness in water repellency.

In 1756, J. G. Leidenfrost[8] was the first to note that a liquid droplet cannot wet a hot surface (*e.g.*, a surface temperature greater than 220 °C), but bounces off due to the formation of a thin vapor film under the droplet. Although there were many studies carried out on water contact angle measurements on low surface energy or hydrophobic solid surfaces in the past three decades,[9–15] most of them concentrated on the effects of temperature on surface wettability. Results from these reports indicated that there was extensive disagreement in both sign and magnitude of the contact angle dependence with temperature. Neumann[9] showed that the contact angle of water on a polyamide surface increased with temperature, but Phillips and Riddiford[10] reported that the contact angle of water on the silicone glass surface remained essentially constant at temperatures around 70 °C. Sutula *et al.*[11] reported a temperature coefficient of +0.03° per °C for water on a fluoropolymer. Padday[12] suggested coefficients of −0.15° per °C and +0.55° per °C for advancing and receding contact angles on paraffin wax, at temperatures of 20–40 °C. Petke and Ray[13] suggested that advancing contact angles of water on a series of low surface energy polymers were all negative (0.04–0.14° per °C), while the receding angles could take positive or negative values (−0.04–0.06° per °C). For Teflon surfaces, Neumann[9] observed no variation of the contact angle of water from room temperature to 60 °C under atmospheric pressure, although his results demonstrated coefficients of −0.3° per °C and −0.15° per °C for the butyl chloride, *n*-heptane and butyl alcohol systems.

Other studies have also demonstrated constant water contact angles. These studies include that of Phillips and Riddiford,[10] which reported a constant water contact angle from 0–60 °C for Teflon at 1 atmosphere. The results of Ponter and Boyes[14] also indicated that the contact angle of water remained at 104–105° from 21–100 °C, for smooth PTFE surfaces. The study by Bemardin *et al.*[15] indicated that the water contact angle was constant, at 90°, from 20–120 °C, on aluminum surfaces modified by organic molecules. When the water temperature was greater than 120 °C, the contact angle decreased linearly. This disagreement found for water wettability on these low surface energy hydrophobic surfaces, and water droplet temperatures, suggests that there may be more than one factor contributing to the wettability phenomenon.

Both Liu[7] and Xia[5] *et al.* recently reported that a superhydrophobic surface may lose its ability to repel hot water. From the point of practical applicability, however, a surface that can repel hot liquids may have great potential in industrial applications, such as the high temperature processing of liquid food, water purification, heat transfer, *etc.* Is the loss of water repellency of superhydrophobic surfaces an unavoidable consequence of contact with hot water? Here, we explore the wettability of water from room temperature to 85 °C, on five kinds of superhydrophobic surfaces, held at different temperatures.

# Experimental

Water contact angle (WCA) measurements were carried out on a SL200B Static and Dynamic Optical Contact Angle Goniometer (Shanghai SOLON Information Technology Co., Ltd.). The experimental setup can be found in detail in the ESI (Fig. S1†). The instrument was equipped with a constant temperature sample stage that can be heated to 100 °C. The temperature was measured by using a sensor in the stage surface or by using an IR sensor at the sample surface. Five μL droplets of 18 MΩ water were supplied, by a 100 μL syringe, from a 15 L heated water container. In order to avoid thermal loss of the water droplet on superhydrophobic surfaces, WCA measurements were carried out within 5 seconds. The measurements were performed using a photograph of the shape of the droplet on the surfaces, as illustrated in Fig. S2 in the ESI.† The drop profile, as shown in Fig. S2,† was automatically fit by a program, using the cyclic approximation.

The superhydrophobic surfaces used for our measurements are commercial superhydrophobic and nanocomposite superhydrophobic coatings from Wuxi Shunye Technology, SY-Supercoat-SHPU101 polyurethane, SY-Supercoat-SHOS101 organosilicone, SY-Supercoat-SHTM101 transparent $SiO_2$-based coatings, and SY-Supercoat-SHTM201 transparent $SiO_2$–fluorocarbon resin; poinsettia leaf was also used to represent a natural superhydrophobic surface. To create the nanocomposite coatings from these products, their slurries were spray-cast onto 6 × 14 cm aluminum substrates, using an airbrush. The substrates were coated with a single spray application from a distance of 10–20 cm above the substrate and then heat-cured at 100 °C for 1 h. The film thickness was about 40–50 μm. The SY-Supercoat-SHTM101 and SY-Supercoat-SHTM201 solutions were dip coated, using a glass slide (or Si wafer for XPS measurement) as a substrate, followed by ethanol sonication. The transparent film thickness was about 50–100 nm. The coated thin films were cured at 300 °C and 100 °C, respectively, for 1 h.

XPS was carried out on a PHI 5000 Versa Probe-II, using monochromatic Al Kα X-rays, at an energy of 1486.6 eV. Survey spectra were recorded using 0.8 eV steps, at a pass energy of 100 eV, and high resolution spectra were recorded using 0.05 eV steps at a pass energy of 25 eV.

# Results and discussion

### 1. Surface morphology and composition of the superhydrophobic surfaces

Fig. 1–5 are SEM photomicrographs of the superhydrophobic surfaces. Both red and green poinsettia leaves are found to have similar structures: Fig. 1 shows that they are composed of 5–15 μm protrusions with 5–10 μm separations, made of vertically orientated nanoplates, 20–1000 nm in length and 30–50 nm in thickness. The nanoplates are distributed across the entire leaf surface, both on the bulges and between, separated by distances of 30–3000 nm. In addition, the nanoplates are randomly oriented, intersecting with other nanoplates. In certain locations on the leaf surface, nanoplates were absent (see Fig. S4†). This may have been caused by inadvertent wear.

 

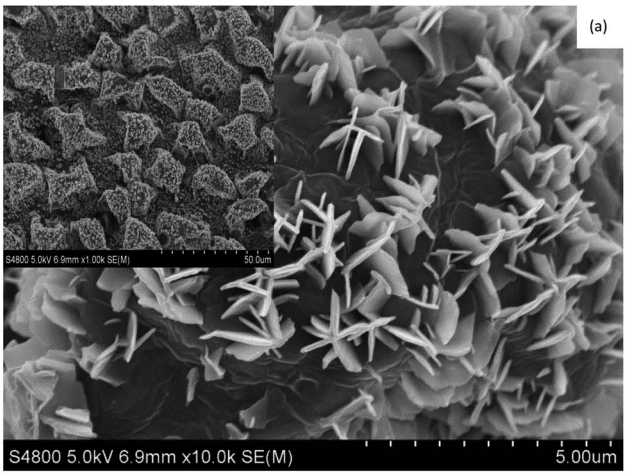


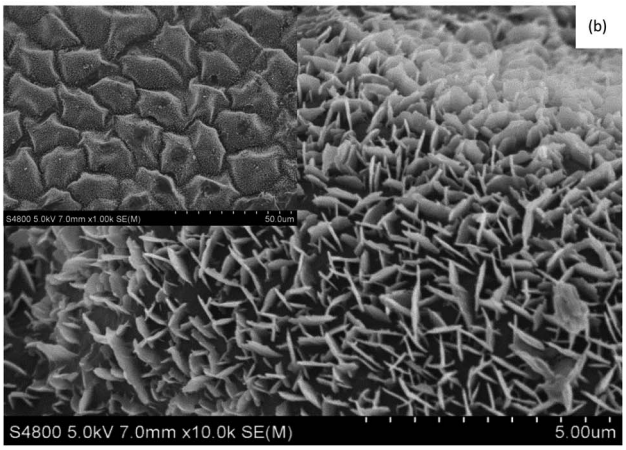


Fig. 1 SEM photomicrographs of (a) red-leafed and (b) green-leafed poinsettia surfaces. Insets are low magnification photographs.

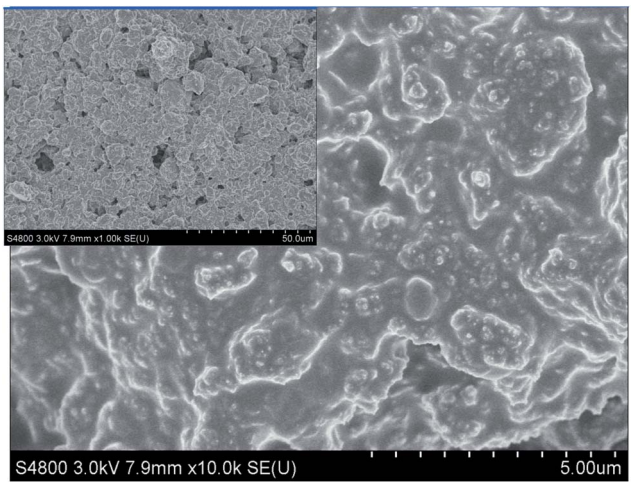


Fig. 2 SEM photomicrograph of OS resin-based superhydrophobic coating. The inset is a low magnification photograph.

Organosilicone (OS) and polyurethane (PU) resin-based superhydrophobic coatings have similar morphologies (see Fig. 2 and 3, respectively): numerous pores enclosed by micro- and nanometer scale microstructures. However, the two transparent superhydrophobic coatings, as shown in Fig. 4 and 5, contain solely densely packed nanoparticles 20–30 nm in size, forming a very smooth surface, compared to the PU and OS resin-based coatings; they have very flat surfaces, with roughnesses less than 8 nm, as measured by using a profiler, while the surface roughness of the PU and OS resin-based coatings can be as high as 3–10 μm.

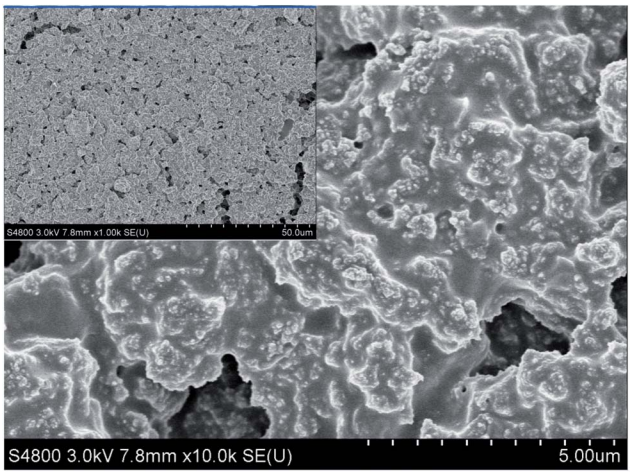


Fig. 3 SEM photomicrograph of PU resin-based superhydrophobic coating. The inset is a low magnification photograph.

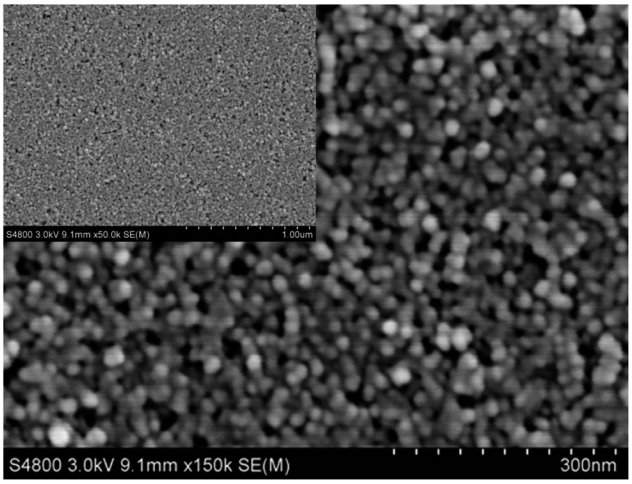


Fig. 4 SEM photomicrographs of $SiO_2$-based (SHTM101) transparent superhydrophobic coating. The inset is a low magnification photograph.

The SHTM201 $SiO_2$–fluorocarbon resin coating has a higher porosity than SHTM101 does. Despite this, both samples have transmittance above 92%, indicating antireflection properties.

XPS survey spectra of all the coatings can be seen in Fig. S6,† and their surface chemical compositions, estimated by the relative sensitivities of the XPS peak areas, are shown in Table 1. C1s high resolution XPS is shown in Fig. S7† (the PU resin-based nanocomposite coating data are not included because they are essentially identical to the OS resin-based coating data). Only

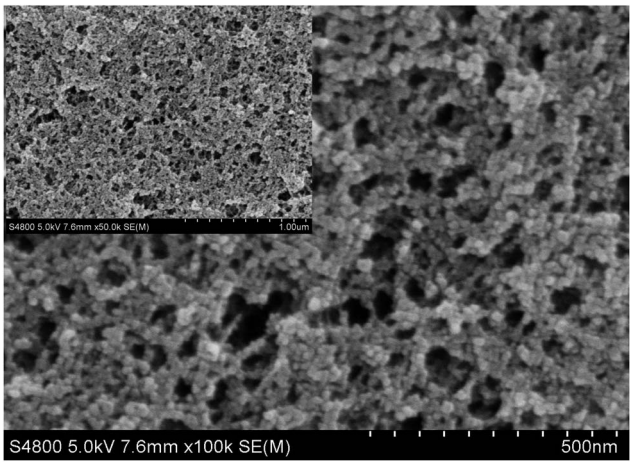


Fig. 5 SEM photomicrographs of $SiO_2$–fluorocarbon resin-based (SHTM201) transparent superhydrophobic coating. The inset is a low magnification photograph.

Table 1 Surface chemical composition of different coatings by XPS (at%)

| Samples | C | O | Si | F |
|---|---|---|---|---|
| SHTM101 | 26.7 | 39.8 | 33.5 | 0 |
| SHTM201 | 29.2 | 36.0 | 30.0 | 4.6 |
| SHOS101 | 47.7 | 6.3 | 1.4 | 44.6 |
| SHPU101 | 46.4 | 7.8 | 1.2 | 44.6 |

C–C/C–H bonds are present at the TM101 superhydrophobic coating surface, while both TM201 and OS/PU resin-based superhydrophobic surfaces also contain $-CF_3$, $-CF_2$, and $-C-CF_2$ bonds.

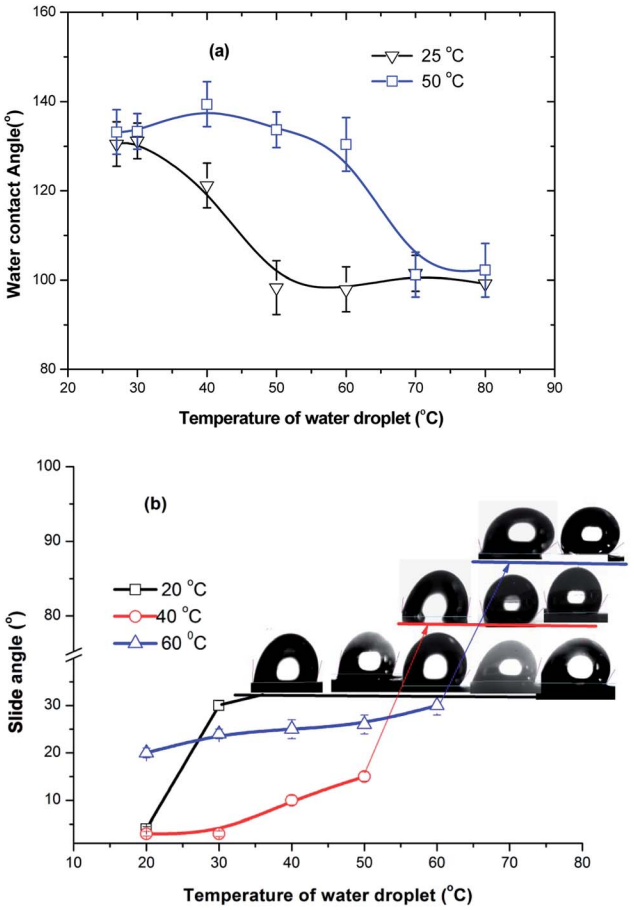


Fig. 6 (a) Water contact angle and (b) slide angle, as a function of water droplet temperature on red-leafed poinsettia at different surface temperatures. The data appearing as droplet photographs indicate conditions under which the drops adhered to the surface, obviating slide angle determination.

## 2. The wettabilities of water droplets, at different temperatures, on surfaces at different temperatures

All measurements of water contact angles, on both red- and green-leafed poinsettias, both front and back, demonstrated elevated water repellency with 130–150° contact angles and 2–40° slide angles at room temperature. Fig. 6a shows the water contact angle of the red-leafed poinsettia, as a function of water droplet temperature, at 25 and 50 °C surface temperatures, while Fig. 6b shows the water slide angle of the red-leafed poinsettia, which varies with water droplet temperature at 20, 40 and 60 °C surface temperatures. Although the number of surface temperatures used is limited, the results indicate that the water repellency, regardless of the water droplet temperature, is reduced when the poinsettia leaf surface temperature is lower than that of the water droplet. A plot of the WCA as a function of water droplet temperature, for lotus leaf surfaces held at room temperature, showed a similar trend.[7] This trend also applies to leaves at elevated temperatures, which resulted in water repellency: a high WCA and slide angle were maintained until the temperature of the water droplet exceeded 60 °C. It should be noted that the nano-wax surface structures of both the red and blue leaves have been damaged after hot water droplet contacting (*e.g.*, 80 °C during test) (see Fig. S4f†).

Fig. 7–10 illustrate the repellency of water droplets as a function of surface temperature. The data from all three superhydrophobic surfaces have similar trends: the WCA remains constant with temperature until that of the surface is reached, whereupon it decreases with increasing droplet temperature. The greater the surface temperature, the smaller the slide angle. That is, the surface remains superhydrophobic as long as its temperature is higher than that of the droplet. It is also interesting to note that, in the case of the high transparency coating surface, there is only a small loss of superhydrophobicity (see Fig. 9 and 10).

All things considered, the reaction of a superhydrophobic surface to hot water can be classified in two ways: (a) water repellency is maintained when the surface temperature is higher than that of the hot water, typical of Cassie–Baxter wetting (see Fig. 11a); (b) water repellency is reduced when the surface temperature is lower than that of the water droplet, typical of Wenzel wetting (see Fig. 11b).

 

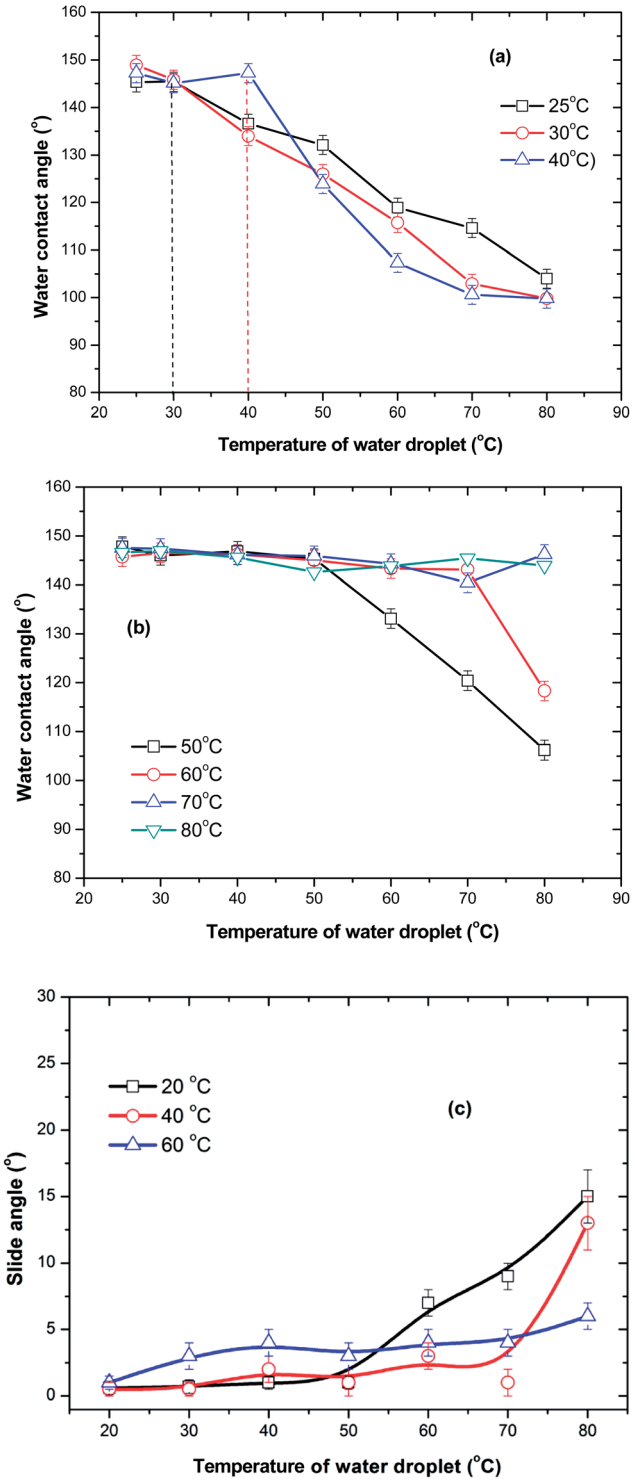


Fig. 7 Dependence of (a and b) water contact angle and (c) slide angle on the temperature of the water droplet for several OS resin-based coating surface temperatures.

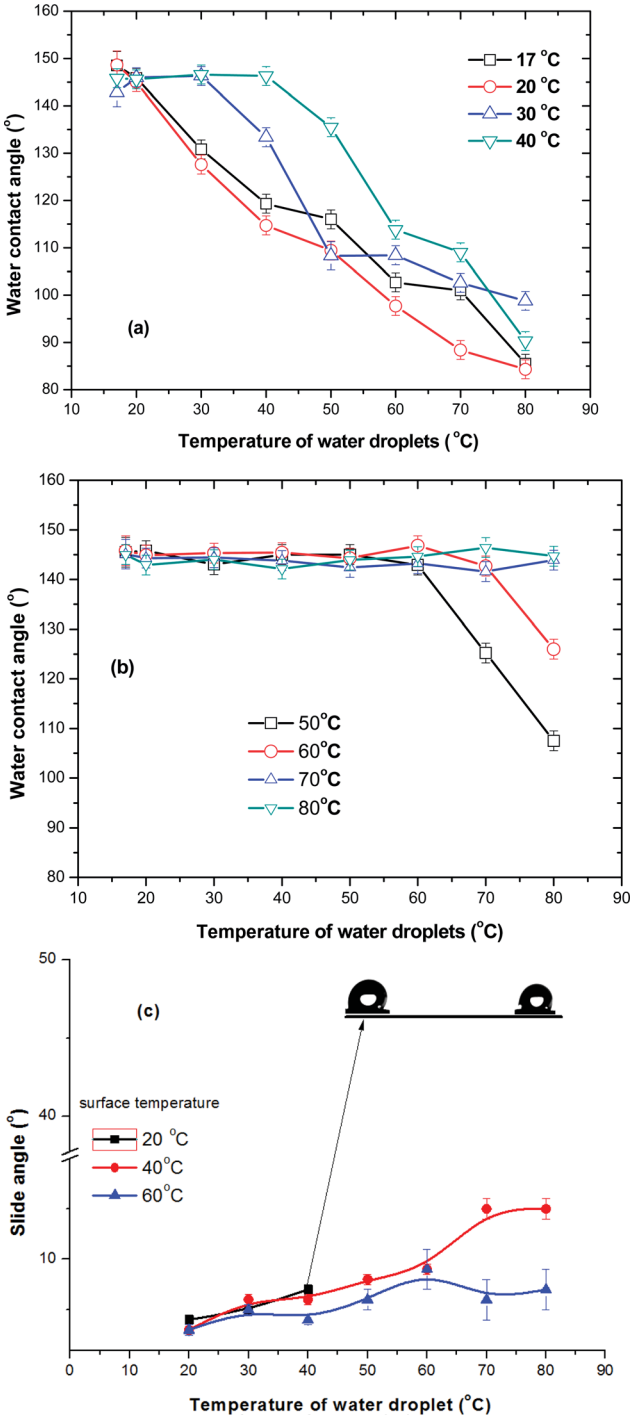


Fig. 8 Dependence of (a and b) water contact angle and (c) slide angle on the temperature of the water droplet for several PU resin-based coating surface temperatures.

The water contact angle of a droplet on a solid surface is typically described by Young's equation (1):

$$\cos\theta = (\gamma_{sa} + \gamma_{sl})/\gamma_{la}, \quad (1)$$

where $\gamma_{sa}$, $\gamma_{sl}$ and $\gamma_{ls}$ are, respectively, the solid–air, solid–water and air–water interfacial surface tensions. A relationship between the apparent and true water contact angle for the droplets on porous surfaces has been established by Cassie and Baxter:[16]

$$\cos\theta_A = f_1 \cos\theta - f_2, \quad (2)$$

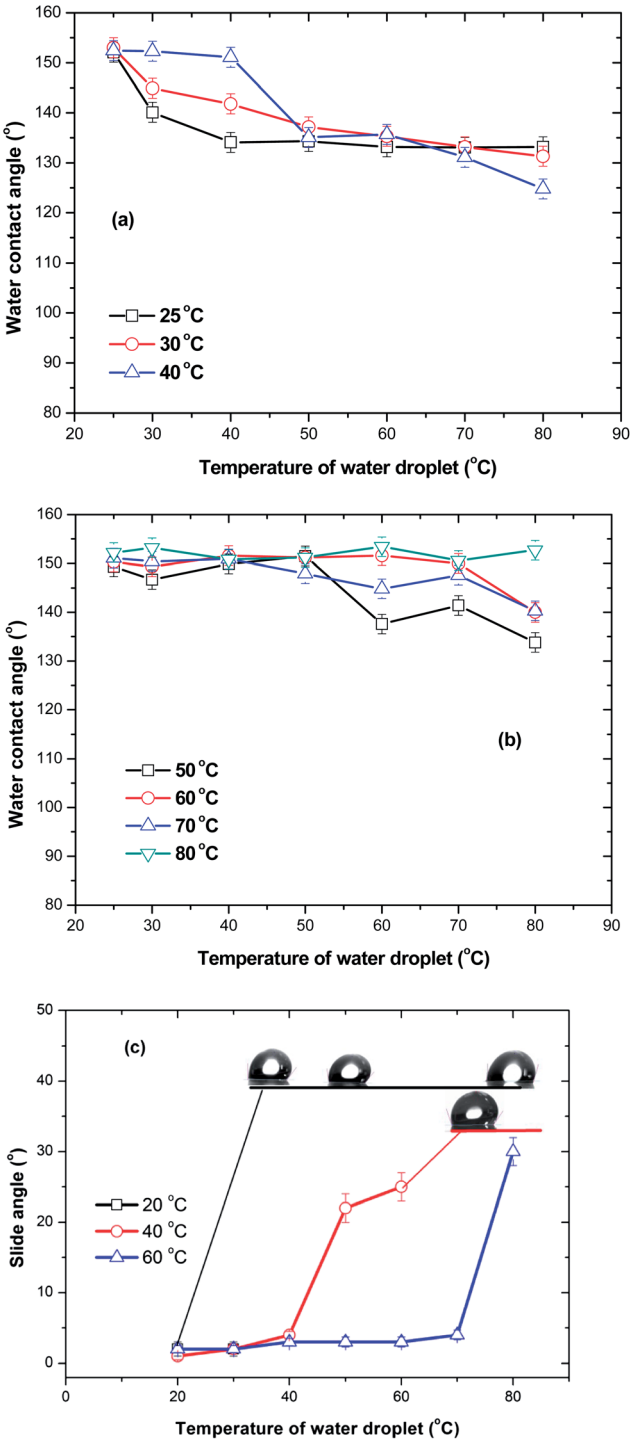


Fig. 9 Dependence of (a and b) water contact angle and (c) slide angle on the temperature of the water droplet for several transparent superhydrophobic coating (TM101) temperatures. The data appearing in the inset indicate conditions under which the drops adhered to the surface, obviating slide angle determination.

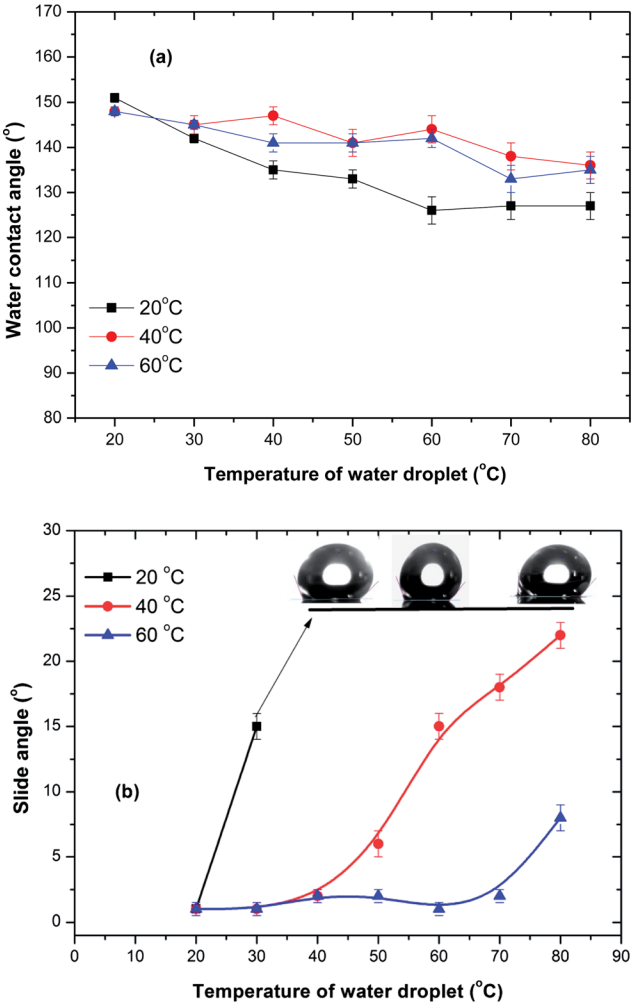


Fig. 10 Dependence of (a) water contact angle and (b) slide angle on the temperature of the water droplet for several transparent superhydrophobic coating (TM201) temperatures. The data appearing as droplet photographs indicate conditions under which the drops adhered to the surface, obviating slide angle determination.

where $\theta_A$ is the apparent contact angle, $f_1$ is the area of the solid–water interface, and $f_2$ is the apparent area of the air–water interface. The equation shows that $\theta_A$ will be larger than $\theta$ when $f_2$ is positive, *i.e.*, when an additional air–water interface is formed. This equation is considered to be the basis for surface roughness-induced superhydrophobicity. From eqn (1) and (2), the influence of the droplet temperature on water contact angles is mainly controlled by $\gamma_{ls}$ and $f_2$. Considering the fact that the surface tension decreases with increasing water droplet temperature:[14,17]

$$\gamma = 75.714 - 0.1414t - 0.25399 \times 10^{-3}t^2, \quad (3)$$

where $\gamma$ is the surface tension of water at temperature $t$ (°C). According to eqn (3), the surface tension of water at 25 °C (~72 dyn cm$^{-1}$) drops to 66 dyn cm$^{-1}$ when the temperature of water is 60 °C. Obviously, the water contact angle will also decrease, according to eqn (1). How this affects the contact angle is unknown because previous experimental studies indicated that there is minimal influence[9,14,15] of the water contact angle on low energy surfaces, *e.g.*, PTFE. Therefore, the dependence of water droplet temperature on $f_2$ (additional water–air interfaces) may play an important role in the effect of hot water on the surface wettability of superhydrophobic surfaces.

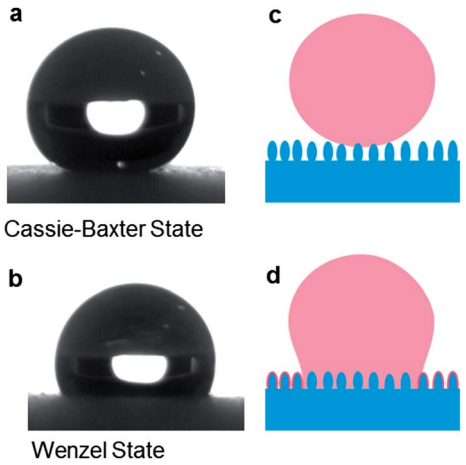


Fig. 11 Photographs of water droplets on the superhydrophobic surfaces when the water droplet temperature is (a) lower than and (b) higher than that of the surface. Included are schematic representations (c and d) of the two states, with the red lines in (d) representing water molecules adsorbed at the water–air interface and nearby the water droplet surface.

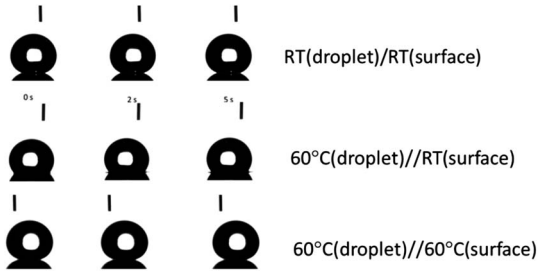


Fig. 12 Initial stage (<5 s) time lapse photographs of water droplets on the transparent coating surface, for several surface and water temperatures.

It is well-known that water molecules adsorb onto a solid surface when the surface temperature is lower than that of the droplet. These adsorbed water molecules then cause the surface to lose its superhydrophobicity, and become hydrophilic, instead.[18–20] For our superhydrophobic coating surfaces, the change experienced by the water droplets on the superhydrophobic surfaces, transitioning from Cassie–Baxter to Wenzel wetting, is illustrated in Fig. 11. The water contact angle will decrease, while the slide angle will increase as water droplets adhere to the surface when its temperature falls below that of the water because there will be water molecules already adsorbed on the surface. Both air trapped under the water droplet and around it, and the new hydrophilic surface that results from water molecule adsorption will then give rise to a decreased water–air interface ($f_2$). This will lead to a decrease in the WCA, due to a decrease in $f_2$ in eqn (2). The lower the temperature of the superhydrophobic surfaces, the smaller the hot water contact angle (or the larger the slide angle) on the surfaces will be. This is also confirmed by the observation shown in Fig. 12, which is a series of time-lapse photographs of the evaporation (<5 s) of a hot water droplet on the relatively low temperature surface of our transparent superhydrophobic coating. The faint horizontal line, seen in the 2 s time lapse photograph for the 60 °C droplet on the RT panel, is the fog of evaporated water molecules (which can also be seen from our video in the ESI,† the fog formation following a droplet leaving the superhydrophobic surface).

However, there is no clear evidence that how the surface physical chemistry affects the wettability of hot water. We have provided two very smooth transparent superhydrophobic surfaces in this work. The TM201 (containing some fluorocarbon) surface showed a greater superhydrophobicity to hot water than did the TM101 coating surface, which may be attributed to the lower surface tension of TM201 compared to TM101. Both the XPS and SEM results for the essentially identical chemical composition and surface roughness of the PU and OS resin-based nanocomposite coatings (Fig. 2, 3 and Table 1) make it difficult to explain their experimental differences in both the WCA and slide angle as a function of surface and water temperatures. The two superhydrophobic surfaces show a slight difference in the wettability to hot water (Fig. 7c and 8c). Based on Fig. 2–10, we can conclude that there will be a smaller decrease in WCA for a smoother SH surface (pure nanostructures) with water droplet temperature. In order to determine the effect of morphology on surface absorption, we will shortly begin experiments based on well-defined surface structures.

## Conclusions

We have investigated the hot water wettability of superhydrophobic surfaces, using poinsettia leaves, and both commercial resin-based and transparent nanoparticle superhydrophobic coatings. We found that there are two situations a superhydrophobic surface may experience: (a) maintaining Cassie–Baxter wettability by repelling water when the surface temperature is greater than that of the water and (b) transitioning to Wenzel wettability when the surface temperature is less than that of the water. This change of surface superhydrophobicity may be attributed to water molecule adsorption caused by the cooler temperature of the solid surface. This ability to change the superhydrophobicity of a solid surface may be useful in practical applications, such as in heat transfer in industrial processes.

## Acknowledgements

The authors express their appreciation to Wuxi City Technology Innovation foundation for support. J.Y.Y. is grateful to Wuxi Shunye Technology for providing support. T.T.I. is grateful for the financial support of the Office of Competitive Research Funds (OCRF) at King Abdullah University of Science and Technology (KAUST), under the "Competitive Research Grant" (CRG) program.

## References

1 (*a*) X. Zhang, F. Shi, J. Niu, Y. G. Jiang and Z. Q. Wang, *J. Mater. Chem.*, 2008, **18**, 621; (*b*) F. Xia and L. Jiang, *Adv. Mater.*, 2008, **15**, 2482.

2 B. Bhushan and Y. C. Jung, *Prog. Mater. Sci.*, 2011, **56**, 1.
3 (*a*) E. Bormashenko, O. Gendelman and G. Whyman, *Langmuir*, 2012, **28**, 14992; (*b*) Y. Y. Liu, J. H. Xin and C.-H. Choi, *Langmuir*, 2012, **28**, 17426.
4 B. Bhushan, *Langmuir*, 2012, **28**, 1698.
5 F. Xia, H. Ge, Y. Hou, T. Sun, L. Chen, G. Zhang and L. Jiang, *Adv. Mater.*, 2007, **19**, 2520.
6 M. He, H. Li, J. Wang and Y. Song, *Appl. Phys. Lett.*, 2011, **98**, 093118.
7 Y. Y. Liu, X. Q. Chen and J. H. Xin, *J. Mater. Chem.*, 2009, **19**, 5602.
8 M. Nosonovsky and B. Bhushan, *Multiscale Dissipative Mechanisms and Hierarchical Surfaces*, Springer, Berlin Heidelberg, 2008, ch. 9.
9 A. W. Neumann, *Proc. Fourth Internat. Cong. Surface Activity*, Brussels, 1964.
10 M. C. Phillips and A. C. Riddiford, *Nature*, 1965, **205**, 1005.
11 P. A. Sutula, R. Hantola, B. Dalla and L. A. Michel, Abstr. 153rd Meetings Amer. Chem. Soc., 1967.
12 J. F. Padday, *J. Colloid Interface Sci.*, 1968, **28**, 557.
13 F. D. Petke and B. R. Ray, *J. Colloid Interface Sci.*, 1969, **31**, 216.
14 A. B. Ponter and A. P. Boyes, *Nature (London), Phys. Sci.*, 1971, **231**, 152.
15 J. D. Bemardin, I. Mudawar, C. B. Waish and E. I. Franses, *Int. J. Heat Mass Transfer*, 1997, **40**, 1017.
16 A. B. D. Cassie and S. Baxter, *Trans. Faraday Soc.*, 1944, **40**, 546.
17 G. Loglio, A. Ficalbi and R. Cini, *J. Colloid Interface Sci.*, 1978, **64**, 198.
18 K. A. Wier and T. J. MacCarthy, *Langmuir*, 2006, **22**, 2433.
19 H. Ghasemi and C. A. Ward, *J. Phys. Chem. C*, 2010, **114**, 5088.
20 Y.-T. Cheng and D. E. Rodak, *Appl. Phys. Lett.*, 2005, **86**, 144101.